Biosensors and Bioelectronics 163 (2020) 112164

Contents lists available at ScienceDirect

Biosensors and Bioelectronics

journal homepage: http://www.elsevier.com/locate/bios

Conformable surface acoustic wave biosensor for *E-coli* fabricated on PEN plastic film

Leonardo Lamanna [a,b,c,*], Francesco Rizzi [a,**], Venkat R. Bhethanabotla [c,1], Massimo De Vittorio [a,b,1]

[a] Center for Biomolecular Nanotechnologies, Istituto Italiano di Tecnologia, Via Barsanti snc, Arnesano, Italy
[b] University of Salento, Department of Innovation Engineering, Campus Ecotekne, Via Monteroni, Lecce, Italy
[c] Department of Chemical & Biomedical Engineering University of South Florida Tampa, USA

ARTICLE INFO

Keywords:
Surface acoustic wave
Conformable SAW device
E.Coli biosensor
AlN thin Film
Polyethylene naphthalate

ABSTRACT

Over the last decades, great effort has gone into developing new biosensor technologies for applications in different fields such as disease diagnosis and detection of pollutants in water and food. Global developments in robotic, IoT technologies and in healthcare sensors require new flexible sensor technologies that are low cost and built from sustainable and reusable or recyclable materials. One of the most promising technologies is based on the development of surface acoustic wave (SAW) flexible biosensors, which are highly reproducible, reliable and wirelessly controllable. This work presents for the first time a novel aluminum nitride (AlN)-based conformable SAW immunosensor fabricated on recyclable polyethylene naphthalate. We apply it to the detection of *E.Coli* using a faster and innovative functionalization method that exploit Protein-A/antibody affinity. A higher sensitivity (Limit of detection-LoD, $6.54*10^5$ CFU/ml) of the Lamb wave traveling on the polymeric device has been obtained in comparison with SAWs traveling on AlN on silicon substrate (LoD, $1.04*10^6$ CFU/ml). Implementation of a finite element method allowed for the estimation of the single *E.Coli* mass of approximately $9*10^{-13}$ g. This work demonstrates the high biosensing potential of flexible polymeric SAW devices for bacteria contamination control in food chain, water and smart packaging.

1. Introduction

Interest in the development of green and biocompatible biosensor platforms using inexpensive and recyclable technologies has increased recently (Boutry et al., 2019; Han et al., 2019). One strategy is based on the use of biocompatible and recyclable polymeric substrates to reduce the cost and develop a new compliant biosensor (Jin et al., 2013; Lamanna et al., 2019b). The exploitation of recyclable plastics for new technology platforms addresses concerns of plastic pollution of the environment. In fact, pollution has become one of the most pressing environmental issues. To this end, polyesters represent the biggest and most promising recyclable plastic class (Soroudi and Jakubowicz, 2013; Venkatachalam et al., 2012) widely used for the development of a green and biocompatible technology, from food packaging to airspace. Materials engineers are developing new and superior polyesters, such as polyethylene naphthalate (PEN), which are applicable, for example, in flexible electronics and thermal blankets used on spacecraft, satellites, and various space instruments (Arkhireyeva and Hashemi, 2002). The development of such green biosensors find application in different fields from molecular medicine to the detection of water and food pollutants and biological warfare agents (Arlett et al., 2011; Chin et al., 2007; Sangroniz et al., 2019).

In particular, the development of biosensors for Internet of Healthcare Things (IoHT) technologies demands the implementation of new compliant, low cost, sustainable, and reusable or recyclable materials (Garcia et al., 2018; Kim et al., 2019; Lamanna et al., 2019b; Mangayil et al., 2017). The biosensor research community is focusing on two main goals: the further miniaturization of devices, in order to analyze smaller sample quantity (Agostini et al., 2018), and the development of flexible and adaptable biosensors (Lamanna et al., 2019a; Lee et al., 2018). The exploitation of compliant devices is paving the way to the introduction of such sensors in a new generation of medical devices and new, smart

* Corresponding author. Center for Biomolecular Nanotechnologies, Istituto Italiano di Tecnologia, Via Barsanti snc, Arnesano, Italy.
** Corresponding author.
E-mail addresses: leonardo.lamanna@iit.it (L. Lamanna), francesco.rizzi@iit.it (F. Rizzi).
[1] These authors jointly supervised this work.

https://doi.org/10.1016/j.bios.2020.112164
Received 25 November 2019; Received in revised form 19 March 2020; Accepted 20 March 2020
Available online 2 April 2020

packaging with the capability of infection and contamination control checks, such as in smart catheters and food smart packaging. Detection of pathogenic agents such as bacteria, fungi, and viruses, widely present in all the environments is of great interest, in this regard (Xu, 2012).

Escherichia coli represents one of the most widespread contaminants and an important cause of gastrointestinal disease that can include complication such as hemorrhagic colitis and hemolytic–uremic syndrome (Paton et al., 2000) and infection in urological catheters (Foxman, 2010). For instance, Food and Drug Administration (FDA) and European Medicines Agency (EMA) have established microbiological standard limits for water and food safety (Moll et al., 2007). Therefore, in the food chain control and packaging (Jasson et al., 2010), there is a pressing need for such low cost and low power consuming biosensors, which are easy to use with the final goal of applying them in large scale microbiological screening (Agostini et al., 2018; Bashir, 2004) for use in both developed and developing countries.

The standard techniques for pathogen detection are: selective culture and colony counting, polymerase chain reaction (PCR) analysis and immuno-based assays. Such techniques have high reliability and reproducibility with the capability of single cell detection. However, in spite of their high performance, those techniques have drawbacks such as the need for expert operators and expensive and time-consuming procedures. Among the most common laboratory-based methods, a pure microbiological approach as the biological growth on different selective media requires up to 7 days (Foudeh et al., 2014; He et al., 2017; Howe and Harding, 2000); enzyme linked immunosorbent assay (ELISA) methods, used for the detection of bacteria down to 10^3 cells per ml, are slow as incubation and washing steps are necessary and they need an expert operator (Hobson et al., 1996); PCR can detect bacteria down to 10 cells per ml, but the commercially available BAX PCR systems show a limit of detection of 10^4 CFU per ml and are not yet sufficiently rapid as they require between 24 and 26 h (Bailey, 1998). Therefore, over the last decades, miniaturized biosensors have become a promising alternative thanks to their quick response, cost-effectiveness, and manageability (Konry et al., 2012; Xu, 2012). The available devices are based on optical detection, cantilevers and quartz crystal mechanical detection. In spite of the good performance of the available devices, they typically necessitate bulky ancillary instrumentation and/or non-trivial optical alignment with resulting high costs (Agostini et al., 2018; Enosawa et al., 2003; Fritz et al., 2000). A different class of biosensors is based on electrical readout (*e.g.*, impedance sensors, piezoelectric and piezo resistive devices); these devices and their control units are generally more compact, could allow a real time detection but have the drawback of being less sensitive than those based on optical detection (Agostini et al., 2018).

Nowadays, one of the most promising alternative technology in the development of biosensors is based on surface acoustic wave (SAW) microelectromechanical systems (MEMS) (Rocha-Gaso et al., 2009). The value of these devices derives from their intrinsic electromechanical piezoelectric transduction, which guarantees high reliability and reproducibility (Brand et al., 2015). Moreover, thanks to their extremely low power need, they become wirelessly controllable, an essential feature in the development of radio-frequency identification devices (RFID), widely exploited in the food supply chain and in a large-scale fine-monitoring of water (Lamanna et al., 2019b; Niu et al., 2019).

The SAW devices can be divided into three different categories depending on the surface waves exploited: shear horizontal/Love wave (SH-SAW) sensors, Rayleigh wave (R-SAW) sensors and Lamb wave (L-SAW) sensors. Owing to their in-plane deformation, SH-SAWs are exploited for sensing in a liquid environment, allowing real-time detection (Li et al., 2017). R-SAWs, in contrast, are widely used in the development of gas sensors, because of a higher mass loading sensitivity, but they are not suitable for the detection in a liquid environment due to damping of the SAWs (Agostini et al., 2018). Finally, L-SAWs travel within the piezoelectric layer and are typically observed in suspended membranes, that are fragile and difficult to manufacture, or on thin piezoelectric layers deposited on polymeric substrates. They can be exploited in a liquid environment with the advantage of a high phase wave velocity with respect to the previous SAW modes (Fu et al., 2017).

Several utilizations of SAW devices for bacterial sensing are reported in the literature. Many of these are based on thick piezoelectric crystals of materials such as $LiNbO_3$, quartz or $LiTaO_3$ (Kim et al., 2012; Moll et al., 2007). The high electromechanical coupling of these materials has allowed the development of high performance devices despite bulky dimensions, high stiffness, and high material cost. In recent years, improvements of the sputtering deposition process for thin piezoelectric materials has been the driving force for the development of thin film SAW devices based on zinc oxide (ZnO) and aluminum nitride (AlN) grown on rigid substrates, usually silicon (Fu et al., 2017). These materials have the benefit of easy integration in a lab on chip systems at low cost (Fu et al., 2017; Zhou et al., 2015).

The new challenge is the development of a flexible and compliant SAW biosensor for the type of applications mentioned earlier in this introduction. Polyvinylidene fluoride (PVDF), the most promising polymeric piezoelectric material so far, not yet resulted in the development of flexible SAW devices; in fact, no SAW devices based on PVDF have been reported to date. Fortunately, innovations in the deposition techniques have allowed the development of a few flexible SAW sensors based on AlN and ZnO on polymeric substrates, so far demonstrated in thermomechanical sensing by us and others (Jin et al., 2017; Kao et al., 2003; Lamanna et al., 2019b). The development of such a conformable polymeric device, thanks to the recyclability and cost complexity reduction, by virtue of passive wireless operation, will be relevant in large scale applications such as smart packaging in food chain control, bathroom fixture contamination control, and bioreactor control in fermentation plants. In fact, these applications need inexpensive biosensor to be applied on surfaces, without the necessity of a low LOD bacteria detection and a specific surface design.

In this work, our conformable and transparent AlN based SAW device on recyclable PEN substrate (Lamanna et al., 2019b) is improved, and developed into a bacterial biosensor. We demonstrate the high sensitivity of the L-SAWs (Fu et al., 2017) on the polymeric substrate with the sensitivity of the R-SAWs on the silicon substrate for the detection of *Escherichia coli* after drying. We also present a finite element method to understand the change of eigenfrequency in relation to the mass loading, to estimate the mass of a single cell of *Escherichia coli* from our device measurements.

2. Materials and methods

2.1. SAW biosensor

AlN based SAW delay line devices were fabricated on 125 μm thick conformable polyethylene naphthalate (PEN), purchased from Teonex (code Q65HA) with one pretreated surface which improves the growth adhesion (Teonex®), and on rigid silicon substrates for this biosensor development. Details of AlN growth and characterization on PEN have been reported previously (Lamanna et al., 2019b) showing high C axis orientation, and an effective piezoelectric coefficient of 3.3 p.m. V^{-1}. In this work, the microfabrication process has been improved using AZ 5214 image reversal photoresist for a lift-off process with an aluminum deposition of 100 nm carried out with an E-beam evaporator. The lift-off process has the benefit of preserving the AlN surface, important for the enhancement of SAW propagation with respect to the dry plasma etch treated surface. Besides, aluminum has lower density and lower acoustic impedance with respect to molybdenum, providing an improvement in the surface acoustic energy confinement (Fu et al., 2017). Each device has been designed with two identical interdigital transducers (IDTs) consisting of 40 pairs of fingers with a wavelength of 20 μm and a metallization ratio of 0.5. The acoustic aperture was fixed at 20 λ with a distance between the two IDTs of 20 λ. The devices were connected to the VNA (Agilent 8753ES) with a coplanar |Z| Probe with 150 μm pitch.

For the sensing application, the R-SAWs were exploited on the silicon substrate and the L-SAWs on the PEN substrate. These two different modes have been chosen because, as reported in (Lamanna et al., 2019b), the Rayleigh wave propagation on soft polymeric substrate shows a spurious signal not useful in biosensing application, likewise for the Lamb wave on silicon.

L-SAWs on AlN have the advantage of higher sensitivity and higher phase wave propagation (around 10000 m/s) (Fu et al., 2017), which increases the working frequency in comparison to the R-SAWs, which have a phase wave propagation of around 5000 m/s. In fact, higher working frequencies lead to better response for similar devices (Fu et al., 2017). Moreover, in future, Lamb-based SAW devices could find application in a liquid environment with the development of a proper microfluidic system in contrast to the R-SAWs (Fu et al., 2017; Pyun et al., 1998).

2.2. E.Coli growth

Escherichia coli K-12 strain was purchased from Carolina Biological Supply Company. The stock culture was inoculated in a flask of Luria–Bertoni (LB) broth purchased from Sigma-Aldrich. Then, it was incubated at 37 °C for 12 h in aerobic conditions (agitation 250 rpm). Subsequently, 100 μl was spread in a petri dish of LB agar and a single colony was chosen to perform all the experiments. An initial growth analysis was performed to ensure that the bacteria are in the exponential phase of growth, and therefore in the best metabolic condition, before performing the biosensing experiments. This characterization was carried out by measuring the optical density (OD) through turbidimetric counts at 600 nm and by the counting of colony-forming units (CFU) in the LB agar Petri dish (supp.). Bacteria for the sensing test were obtained by centrifugation at 4000 rpm for 10 min (Demitri et al., 2017) and resuspension in equal volume of sterile phosphate buffered saline (PBS). This assures a solution containing mainly whole bacteria compared to dead or lysed bacteria and, at the same time, it prevents continuous bacterial growth that occurs in the broth. The starting solution for all the biosensing experiments was set up at $4.02*10^8$ CFU/ml and serially diluted by three times for each measurement point.

2.3. Surface preparation and bacterial immobilization

The fabricated SAW devices, consisting in a stack of substrate/AlN/Al-IDTs, were treated with O_2 plasma (3 min at 100W); such process does not affect the AlN roughness (Rosenberger, 2007). Then immediately soaked in a solution of 2% of 3-aminopropyltriethoxysilane (APTES) and 1% water in pure ethyl alcohol (EtOH) for 1 h at room temperature. After washing with EtOH and drying in N_2 flow, the devices were baked at 100 °C for 15 min (Arkles, 2003). This process allows for organosilanization of the surface for reproducible protein functionalization. After cooling the devices, the delay lines were soaked in a solution of 3% terephthalaldehyde (TA) in EtOH for 1 h and then washed with EtOH and dried in N_2 flow, where TA works as the crosslinker between the organosilanizated surface and protein (Li et al., 2017). Finally, Protein A (PrA) was conjugated to the surface using a solution of 50 μg/ml at RT for 1.5 h (Fig. 1). PrA is used for the affinity-based antibody immobilization; it has a high affinity and binding specificity towards the antibody Fc region and promotes the high orientation association of the antibody, preventing the denaturation and the lack of orientation associated with the physical and covalent antibody immobilization (Rusmini et al., 2007). After washing thrice with PBS, non-specific binding was prevented by blocking sites on the surfaces with 0.5% bovine serum albumin (BSA) in PBS for 20 min at RT (Brorson, 1997; Xiao and Isaacs, 2012). All the functionalization process requires about 4–5 h.

Two different immune-immobilization approaches have been investigated using polyclonal antibody (Isotype IgG purchased from Bio-Rad Laboratories, Inc.). The first preliminary approach is based on the antibody grafting on the SAW devices and subsequent antibody bacteria interaction. 50 μg/mL anti-*E.Coli* antibody was assembled on the surface of the SAW device for 45 min at RT. Subsequently, the *E. Coli* resuspension was loaded on the device. After 1.5 h, the device was thoroughly rinsed with PBS and subsequently with deionized water, for the removal of the non-specifically bound cells and salts, respectively. The process is completed with drying in a vacuum chamber at 36 °C. This approach has shown low bacteria immobilization on the sensor surface, despite this kind of interaction usually being exploited in ELISA tests and different biosensors (supplementary). Other research groups have faced this problem and the main reason can be attributed to the roughness of the surface. In particular, Moll et al., (2007) show that a surface roughness of around 8 nm, similar to that of our device (Lamanna et al., 2019b), explains this issue. To overcome this problem a second approach was successfully investigated. It consists in a pre-incubation of the *E. Coli* resuspension with the antibody at a final concentration of 50 μm/ml for

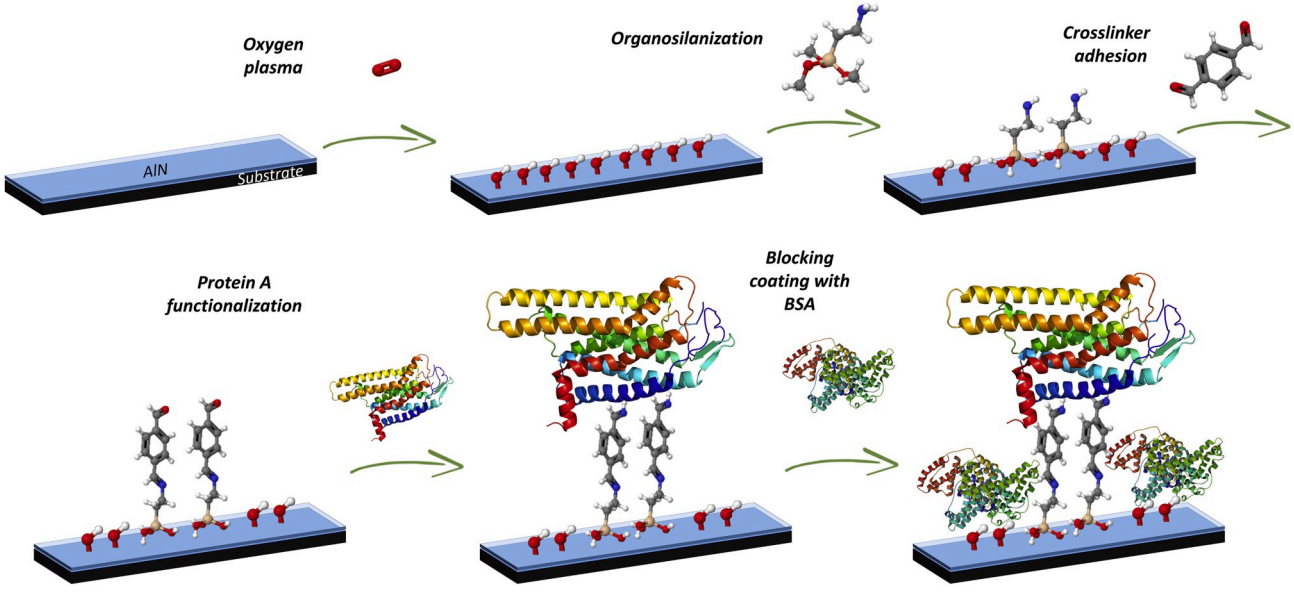

Fig. 1. Processing steps of surface functionalization: hydroxylation using O_2 plasma; organosilanization with APTES; surface activation using crosslinking agent TA; Protein-A functionalization and blocking coating with BSA.

30 min at 36 °C and then the loading of the solution on the SAW devices for 45 min followed by the PBS and DI water washing. The process is completed with drying in a vacuum chamber at 36 °C. This approach enables a higher bacteria immobilization due to an enhancement of the interaction between the antibodies and bacteria in a volumetric reaction and a lower hindrance with PrA and the antibody Fc region. Moreover, this approach shows 1h time-saving, an important feature in a biosensor. The total time required for analyzing one sample is of 1.5h. As a control test, the *E.Coli* resuspensions without antibody were loaded on the devices, to evaluate the nonspecific binding of the bacteria cells with the surface. All the devices have been used within 24 h from the complete immune functionalization, storing the biosensor at 4 °C, to prevent the antibody denaturation. Noteworthy, the devices were reconditioned after washing (acetone/isopropanol/water) and O_2 plasma (10 min 100W) treatment and successfully reutilized for biosensing at different bacteria concentrations. Such process does not affect the AlN surface and the PEN substrate, resistant to all these solvent (Teonex; Zardetto et al., 2011).

In Fig. 2, surface morphology, acquired by Atomic Force Microscopy (AFM, CSI - Nano-Observer Microscope), before and after the surface functionalization are reported. The roughness of the samples before the functionalization shows a RMS equals to 6.407 nm (skew 0.2194) and 7.623 nm (skew 0.1733) for silicon (Fig. 2a) and PEN (Fig. 2b), respectively. After the functionalization, it has been observed an increase of the surface roughness, in particular a RMS equals to 8.563 nm (skew −0.2132) and 9.617 nm (skew −0.1069) for silicon (Fig. 2c) and PEN (Fig. 2d), respectively. The immobilization of the protein A and BSA onto the activated substrates covers the granular structure of AlN surface and induces an increase of the surface roughness of around 1.6 nm. Such behavior is consistent with the data reported in the literature (Grimaldi et al., 2016; Klein et al., 2003; Shin et al., 2016).

3. Result and discussion

3.1. Microscopic imaging

The bacteria adhesion on the SAW devices was verified by optical microscopy and scanning electron microscopy (SEM) using the Hitachi SU 70 instrument. All the picture below are referred to the polymeric-based SAW devices and no difference has been observed for the silicon-based devices since the AlN surface roughness is comparable for both the substrates, as demonstrated by AFM analysis. In Fig. 3 a-d, the optical microscopy images show clearly how the exposure of the biosensor at different concentrations of *E.Coli* have a decreasing adhesion rate as concentration decreases. In Fig. 3 e-g, SEM images of the device loaded with a concentration of $1.34*10^8$ CFU/ml show a uniform distribution of the bacteria on the entire biosensor surface at three different magnifications. Finally, Fig. 3h shows a 3D schematic representation of a conformable AlN-based SAW device grafted with *E.Coli* (anti-*E.Coli* conjugations are highlighted in green).

3.2. Electroacoustic response of the SAW devices

Preliminarily, the devices were tested by measuring the transmission amplitude signal S_{21} (Fig. 5a and b). The device fabricated on silicon show one clear resonance mode corresponding to the R-SAW propagation around 250 MHz, while the device fabricated on PEN shows two clear resonance frequencies corresponding to the propagation of the R-SAWs around 180MHz and L-SAWs around 500 MHz. A transmission signal higher than 20 db is observed for the R-SAW and L SAW resonance modes on silicon and PEN substrate, respectively, with an enhancement respect to the previous work (Lamanna et al., 2019b). This improvement is due to the aluminum IDTs obtained by a lift-off process, as explained previously. To better characterize the biosensing properties of our devices, the phase inversion change was taken as a reference to identify the resonance shift due to the *E. Coli* loading change. In the present work, the electromechanical resonance shifts of R-SAWs on the silicon substrate and the L-SAWs on the PEN substrate have been compared for the biosensing of *E. Coli*.

All the devices were tested before the functionalization to record the reference frequencies f_0, after the functionalization and finally after the bacteria cells adhesion. All the spectra were acquired 50 times and averaged by the Agilent 8753ES. For each concentration, 10 devices were tested using both new and reconditioned devices without measuring evident difference. The experimental set up, used to study the electroacoustic response of the SAW devices, is shown in Fig. 4a; in Fig. 4b a representative photo of a conformable PEN-based SAW device is reported.

No significant frequency resonance decrease was observed due to the functionalization step (data not reported) because of the low weight

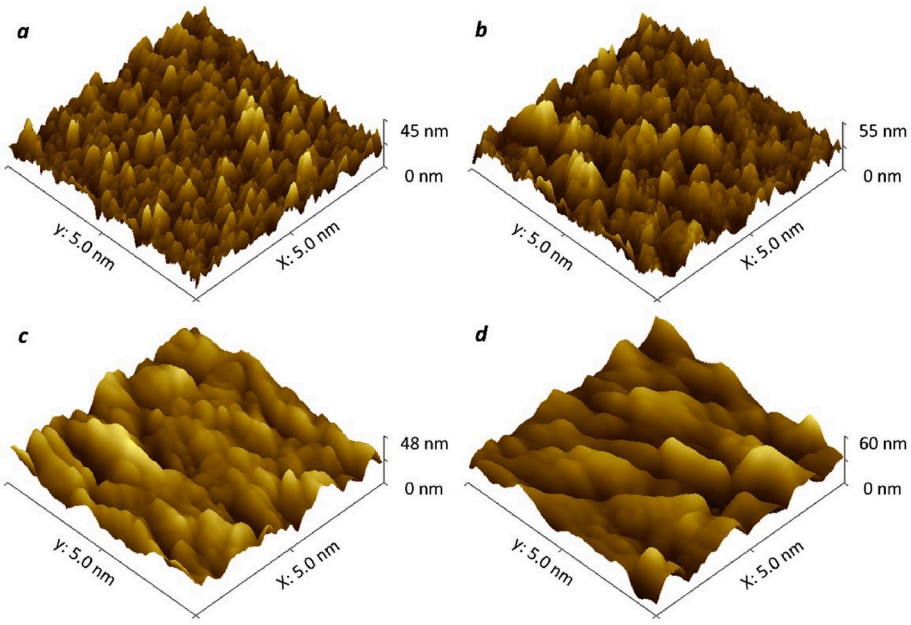

Figure 2. 3D topographic AFM images a,b) AlN surface on Silicon and PEN respectively; c,d) functionalized AlN surface on Silicon and PEN, respectively.

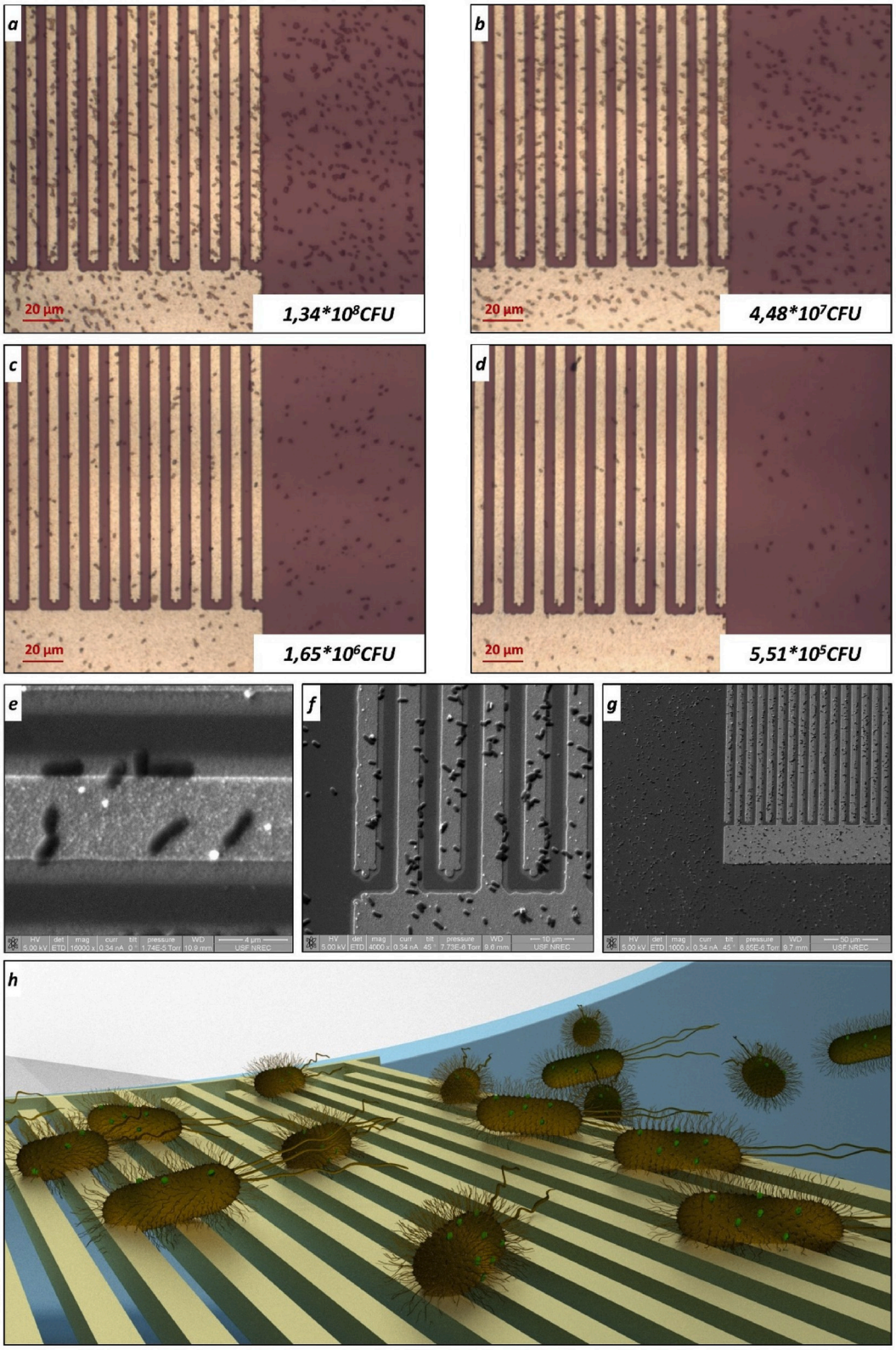

Fig. 3. a-d) optical micrograph of the bacteria adhesion at increasing concentration; e-g) SEM imaging of the grafted bacteria at different magnitude 16k, 4k, and 1k, respectively; h) 3D schematic representation of a flexible AlN-based SAW device grafted with *E.Coli* (anti-*E.coli* conjugations are highlighted in green). (For interpretation of the references to colour in this figure legend, the reader is referred to the Web version of this article.)

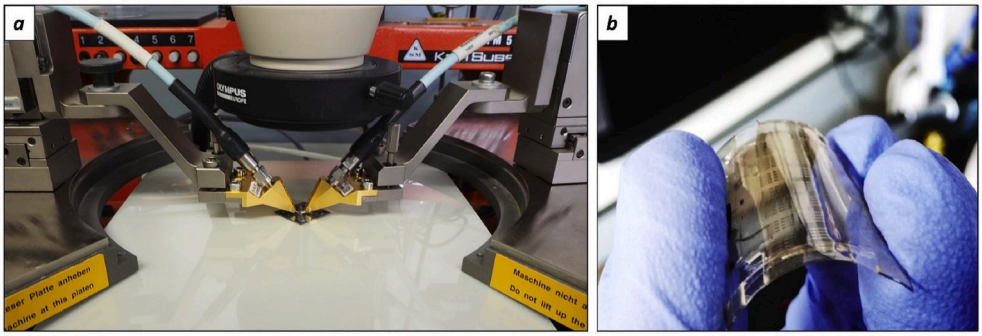

Fig. 4. a) Experimental set up, used to study the electroacoustic response of the SAW devices; b) photo of a conformable PEN based SAW device.

loading of the organosilane-PrA complex (estimated around 10^{-19}g with respect to the bacteria weight, typically estimated around 10^{-12}-10^{-13} g (Kaiser et al., 2007; Moll et al., 2007). Noteworthy, the devices used in the present work have been employed on a fixed substrate, by a PDMS layer, in order to prevent the bending of the device during the measurement, which would generate an unwanted resonance change; moreover, all the devices have been tested in a controlled environment at 25 °C and 30–40% humidity.

In Fig. 5c and d the S_{21} phase curves for silicon and PEN are reported, respectively. A higher frequency shift is observed for the L-SAWs (≈750 kHz) in comparison to the R-SAWs (≈250kHz) due to the higher center frequency and sensitivity of the L-SAWs (Fu et al., 2017). Fig. 5e and f report the resonance frequency shift (f-f_0) as a function of the bacteria concentration for silicon and PEN, respectively. The control experiment results, carried out without the antibody grafting, are shown in the same graphs. The large difference between the measurement and the control curves shows the efficiency of the antibody grafting and adhesion thus proving the responsivity of our biosensor to *E. Coli*. The concentration vs. frequency calibration curve (Fig. 5e and f) is fitted by an interpolation with a sigmoidal curve with an $R^2 = 1$ for both the curve on silicon and PEN substrate (dotted curves in Fig. 5e and f). This fitting curve is exploited to calculate the Limit of Blank (LoB), Limit of Detection (LoD) and Limit of Saturation (LoS) according with *Armbruster* et al. with a 95% confidence interval (Armbruster and Pry, 2008). The values are reported in Table 1.

The experimental LoD of our PEN-based SAW device is equivalent to the detection limit of 10^5–10^6 CFU/ml of SAW devices biosensors presented by other research groups (Rocha-Gaso et al., 2009; Xu, 2012), with the advantage of being a conformable, inexpensive and recyclable biosensor based on polymeric PEN substrate and an AlN thin film as piezoelectric layer. The responsivity to bacteria concentration, in the range of 10^6–10^8 CFU/ml, is extrapolated from the linear regression slope of Δf vs log (CFU): 51.23kHz/log (CFU) with R^2 0.989 and 134.823kHz/log (CFU) with R^2 0.995 for silicon and PEN, respectively (details in supplementary).

The L-SAWs on the conformable PEN substrate show a lower LoD and a higher LoS compared to those reported by many works (Duhamel et al., 2006; Lin et al., 2011; Pyun et al., 1998), confirming the high potential of the L-SAWs exploited in this work on a polymeric substrate. Conformable SAW biosensor could find application, as a disposable device, in the monitoring of biofilm (Flemming and Wingender, 2010; Watnick and Kolter, 2000) and high contaminated environments such as bathroom fixture, industrial fermentation plant and row food chain (fish and meat), where the bacteria concentration is reported to be between 10^5-10^7 CFU/ml (Antwi-Agyei and Maalekuu, 2014; Barker and Jones, 2005; Ranjit and Kung Jr, 2000; Sanjee and Karim, 2016). In this work, all the results have been obtained in a controlled environment but a frequency shift in SAW can depends on temperature, humidity and substrate bending. In future, for the development of a proper conformable SAW biosensor, environmental sensors will be integrated in order to normalize the sensor response in real time.

3.3. FEM modeling

To model how the mass loading due to the bacterial adhesion affects the SAW propagation, a series of 3D simulations have been carried out using the COMSOL multiphysics software. The model used in the previous work (Lamanna et al., 2019b), describing the SAW elemental cell of 2 μm × 20 μm, was implemented with the exploitation of a piezoelectric multiphysics with a further added mass layer describing the bacteria loading influence (Rao et al., 2012); such elemental cell is described in Fig. 6a, where a Rayleigh mode is reported as an example. The system has periodic boundary conditions to dictate that the displacements be the same along both vertical boundaries of the geometry and a fixed boundary condition on the bottom; a tetrahedral mesh has been exploited. A parametric sweep analyses of the added mass density allowed a study of the change of the main superficial wave resonance. The material data used in the FEM model are given in Table 2. This modeling is a good approximation to understand the physics of a SAW device without the necessity of high computing power, needed to simulate the whole device. Such a study allows us to evaluate the overall change of the SAWs propagation eigenmodes in relation with the mass loading. Such model efficiently describes the SAWs propagations eigenmodes in an ideal SAW device under test (DUT) without introducing the delay line (Hao et al., 2016; Li et al., 2019; Rao et al., 2012; Wang et al., 2015).

A top layer of 2 μm was added as a loading layer (Fig. 6a). In particular, we approximated the bacteria adhesion to a slight uniform density increase of this layer according the flowing expression:

$$\rho = N_{bacteria} * \rho_{bacteria} \quad (1)$$

where ρ is added mass density, $\rho_{bacteria}$ is the density supposing there is only one bacteria on the surface of the modeled elemental cell ($\frac{bacteria's\ mass}{volume\ layer}$), with the number of bacteria ($N_{bacteria}$) considered in a range of 0 and 5. In literature, the *E. Coli* mass is reported to be in a range between 10^{-14} g - 10^{-11} g in relation to the strain and the residual water content (Davis et al., 1973; Kaiser et al., 2007; Moll et al., 2007). In this work, the simulations have been carried out supposing a single bacteria mass in the order of 10^{-13} g. A variable water residual percentage content after sample drying has been considered in the simulations by supposing a minimum mass of $2*10^{-13}$ g (dried bacteria) and a maximum mass of $15*10^{-13}$ g (wet bacteria). The number of bacteria were considered to be in the range between 0 bacteria and a maximum of 5 bacteria on the elemental cell of the SAW surface. This latter value covers the entire modeled area and it was speculated by the microscope picture (area highlighted in red in Fig. 6a) and by the dimension of the *E. Coli* (around 2 μm × 0.5 μm) (Allen et al., 2014; Kubitschek, 1990). Fig. 6b and c show the simulated curve of the shift for R-SAWs and L-SAWs for silicon and PEN substrate, respectively. In particular, the upper curves (in red) refer to a mass loading considering a minimum

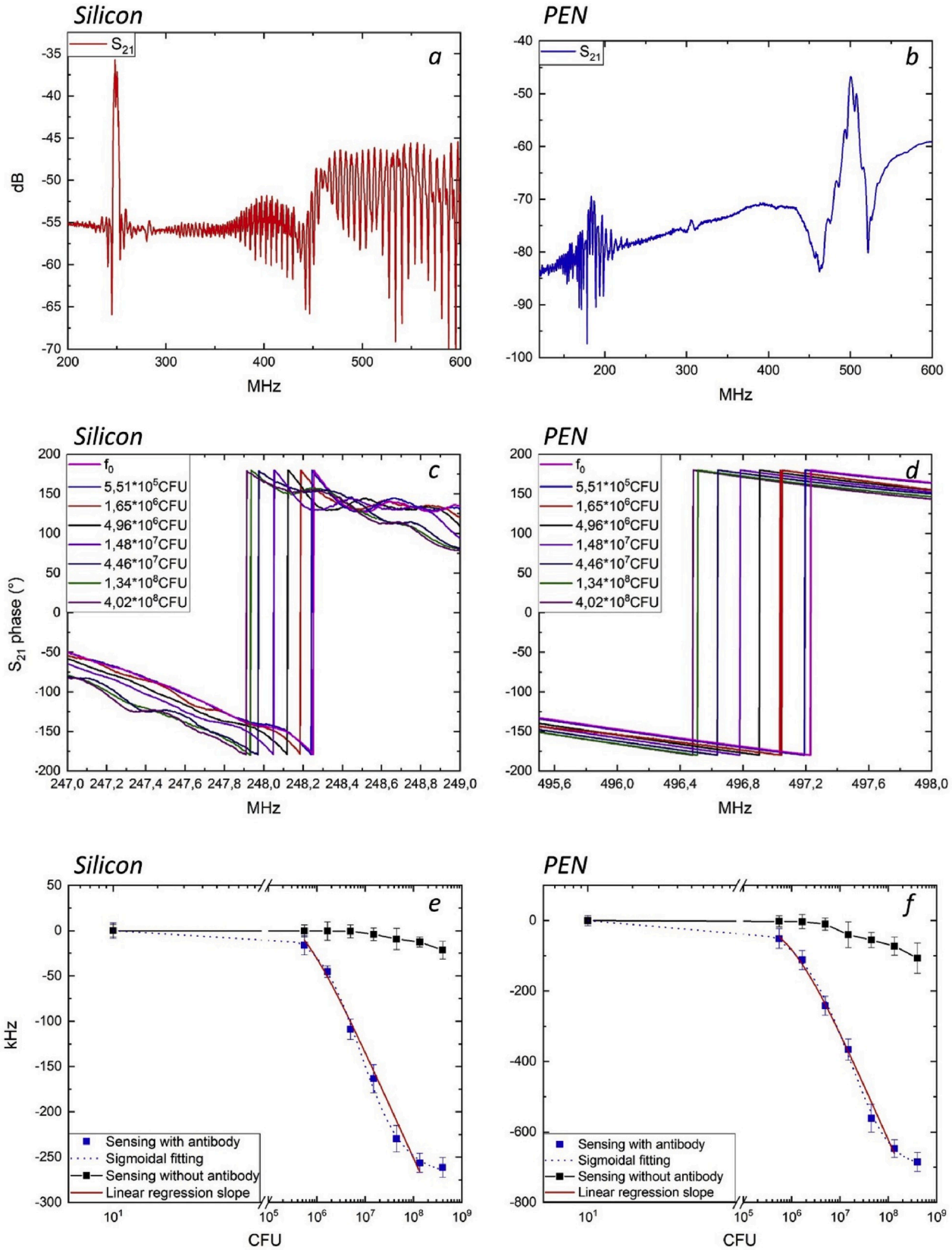

Fig. 5. a,b) Transfer function amplitude S_{21} of AlN based SAW devices fabricated on silicon and PEN substrate, respectively; c,d) S_{21} phase change in relation of bacteria mass loading for silicon and PEN devices respectively; e,f) resonance frequency shift in function to the bacteria concentration, with and without antibody grafting (blue and black respectively), for R-SAWs on silicon and L-SAWs on PEN, respectively. The reported error bars show the standard deviation. (For interpretation of the references to colour in this figure legend, the reader is referred to the Web version of this article.)

Table 1
Comparison of the L-LoB, LoD, and LoS of the silicon R-SAW and PEN L-SAW devices.

Device	LoB (CFU/ml)	LoD (CFU/ml)	LoS (CFU/ml)
Silicon substrate	$4.22*10^5$	$1.04*10^6$	$8.33*10^7$
PEN substrate	$3.91*10^5$	$6.54*10^5$	$1.25*10^8$

bacteria mass of $2*10^{-13}$ g and the lower curves (in black) refer to a maximum bacteria mass of $15*10^{-13}$ g. The experimental curves have been overlaid with the modeled plots, with the supposition to have and adhesion between zero to four bacteria in the analyzed CFU range. In fact, analysis of multiple microscope images excludes the uniform coating or clusters of bacteria on the surface and suggests a maximum number of bacteria equals to 4 in the elemental cell (*e.g.* Fig. 3 a-d). It was observed how in both the case of the silicon and PEN substrate the experimental curve is in the fork traced by the modeled curves of minimum and maximum bacteria's mass (Fig. 6b and c), suggesting an intermediate experimental *E.Coli* mass. Finally, this model was exploited to estimate the *E.Coli* mass. The best fit (dashed line in Fig. 6) was obtained with a mass of $6.16*10^{-13}$ g and $12.61*10^{-13}$ g for rigid silicon and conformable PEN substrates, respectively; which suggests a *E. Coli* mass of approximately $9*10^{-13}$ g.

4. Conclusions

Conventional laboratory-based methods remain the gold standard for bacteria/pathogen detection due to their high sensitivity and selectivity. On the other hand, the necessity of rapid and reliable detection methods, is becoming a driving force for the development of new biosensor technology as witnessed by the surge increase of patent/publication numbers in recent years. In fact, biosensors have great potential of becoming effective in daily measurement tools, wearable sensing and IoT applications thanks to their quick response and portability. Several key challenges, including selectivity, high sensitivity, specificity, and competitive cost, will need to be faced to realize such a competitive biosensor. In this framework, our contribution consists in the development of a novel conformable AlN-based SAW biosensor. The devices were exploited to detect *E. Coli* bacteria. A new approach for

Table 2
Material properties used in the FEM modeling.

Material	Density (Kg/m^3)	Young modulus (GPa)	Poisson ratio
Aluminum	2700	70	0.33
Silicon	2320	160	0.22
PEN	1360	12.2	0.49
AlN	3300	340	0.25
Mass loading cell	P	10	0.48

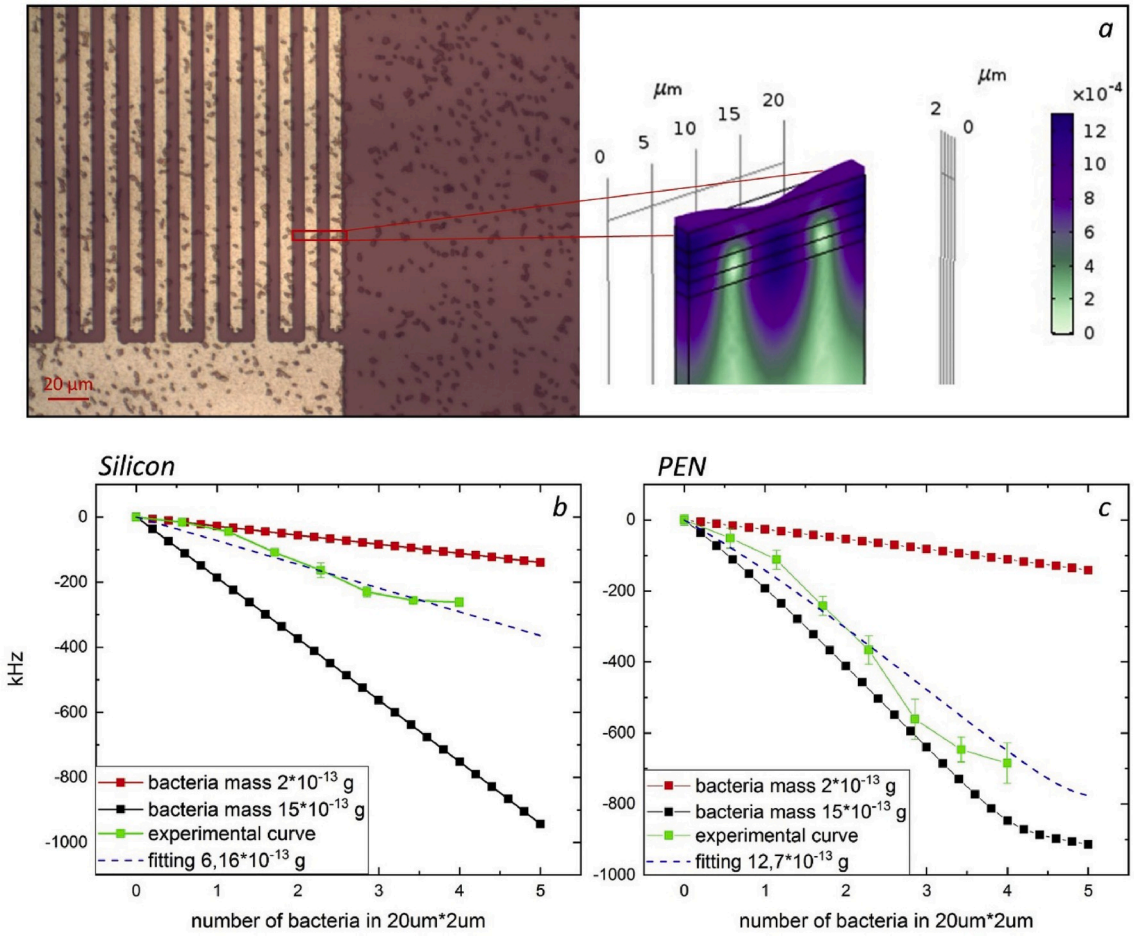

Fig. 6. FEM simulation: a) On the right side it is shown the 3D structure used to perform the COMSOL simulations, corresponding to the red highlighted area in the optical micrograph; b,c) These graphics show the mass parametric sweep analysis of the main surface eigenfrequency, with different bacteria mass loading for silicon and PEN, respectively. The red curves show the theoretical resonance shift due to a single bacteria mass of $2*10^{-13}$g; The black curves show the theoretical resonance shift due to a single bacteria mass of $15*10^{-13}$g; the dashed curves have been obtained by fitting the real data (green slopes) in the FEM model. (For interpretation of the references to colour in this figure legend, the reader is referred to the Web version of this article.)

immunoassay biosensor functionalization is exploited with the advantage of time-saving protocol and improvement in the bacteria adhesion rate on the device. The method consists of Protein-A graft on the surface, followed by the adhesion of *E.Coli* bacteria pre-mixed with anti-*E. Coli* antibody. The results obtained on polymeric L-SAW-based biosensor are compared with a rigid R-SAW-based biosensor. The shift of the resonance frequency in SAW-based biosensor in relation to the bacteria CFU concentration was used as a detection method. The L-SAWs on the PEN substrate show better results as compared to the R-SAWs. In particular, an LoD of $1.04*10^6$ and $6.54*10^5$ and an LoS of $8.33*10^7$ and $1.25*10^8$ have been calculated for silicon and PEN, respectively. FEM simulations were developed to understand the mass loading influence on the SAW propagation modes. Experimental data were represented by the finite element model well, with the *E.Coli* mass estimated as: $6.16*10^{-13}$ g and $12.61*10^{-13}$ g on the rigid and flexible substrates, respectively.

This work represents the first polymer-based conformable SAW device exploited in biosensing. Moreover, the large transmission signal amplitude S_{21} (up to 20 db, sufficient for electronic and communication applications (Jin et al., 2013)) and the combination of two biocompatible materials, AlN and PEN, could pave the way for the development of an inexpensive and recyclable RFID based biosensor to be exploited in the food chain, large-scale fine-monitoring of water and smart packaging for bacteria contamination control.

Declaration of competing interest

The authors declare that they have no known competing financial interests or personal relationships that could have appeared to influence the work reported in this paper.

CRediT authorship contribution statement

Leonardo Lamanna: Conceptualization, Methodology, Formal analysis, Visualization, Investigation, Data curation, Validation, Writing - original draft. **Francesco Rizzi:** Conceptualization, Methodology, Formal analysis. **Venkat R. Bhethanabotla:** Conceptualization, Supervision. **Massimo De Vittorio:** Conceptualization, Supervision.

Acknowledgment

This work was partially funded by the National Science Foundation (Grant No. IIP-1640668), which is gratefully acknowledged.

Appendix A. Supplementary data

Supplementary data to this article can be found online at https://doi.org/10.1016/j.bios.2020.112164.

References

Agostini, M., Greco, G., Cecchini, M., 2018. A Rayleigh surface acoustic wave (r-SAW) resonator biosensor based on positive and negative reflectors with sub-nanomolar limit of detection. Sensor. Actuator. B Chem. 254, 1–7.
Allen, C., Loo, J.F., Yu, S., Kong, S., Chan, T.-F., 2014. Monitoring bacterial growth using tunable resistive pulse sensing with a pore-based technique. Appl. Microbiol. Biotechnol. 98 (2), 855–862.
Antwi-Agyei, P., Maalekuu, B., 2014. Determination of microbial contamination in meat and fish products sold in the Kumasi metropolis (A Case Study of Kumasi central market and the Bantama market). Merit Res. J. Agri. Sci. Soil Sci. 2 (3), 38–46.
Arkhireyeva, A., Hashemi, S., 2002. Fracture behaviour of polyethylene naphthalate (PEN). Polymer 43 (2), 289–300.
Arkles, B., 2003. Silane coupling agents: connecting across boundaries. Morrisville: Gelest 9–12, 2003.
Arlett, J., Myers, E., Roukes, M., 2011. Comparative advantages of mechanical biosensors. Nat. Nanotechnol. 6 (4), 203.
Armbruster, D.A., Pry, T., 2008. Limit of blank, limit of detection and limit of quantitation. Clin. Biochem. Rev. 29 (Suppl. 1), S49.
Bailey, J., 1998. Detection of Salmonella cells within 24 to 26 hours in poultry samples with the polymerase chain reaction BAX system. J. Food Protect. 61 (7), 792–795.
Barker, J., Jones, M., 2005. The potential spread of infection caused by aerosol contamination of surfaces after flushing a domestic toilet. J. Appl. Microbiol. 99 (2), 339–347.
Bashir, R., 2004. BioMEMS: state-of-the-art in detection, opportunities and prospects. Adv. Drug Deliv. Rev. 56 (11), 1565–1586.
Boutry, C.M., Beker, L., Kaizawa, Y., Vassos, C., Tran, H., Hinckley, A.C., Pfattner, R., Niu, S., Li, J., Claverie, J., 2019. Biodegradable and flexible arterial-pulse sensor for the wireless monitoring of blood flow. Nature biomedical engineering 3 (1), 47.
Brand, O., Dufour, I., Heinrich, S., Heinrich, S.M., Josse, F., Fedder, G.K., Korvink, J.G., Hierold, C., Tabata, O., 2015. Resonant MEMS: Fundamentals, Implementation, and Application. John Wiley & Sons.
Brorson, S.-H., 1997. Bovine serum albumin (BSA) as a reagent against non-specific immunogold labeling on LR-White and epoxy resin. Micron 28 (3), 189–195.
Chin, C.D., Linder, V., Sia, S.K., 2007. Lab-on-a-chip devices for global health: past studies and future opportunities. Lab Chip 7 (1), 41–57.
Davis, B., Dulbecco, R., Eisen, H., Ginsberg, H., 1973. Bacterial Physiology: Microbiology. Maryland Harper and Row, pp. 96–97.
Demitri, C., Lamanna, L., De Benedetto, E., Damiano, F., Cappello, M.S., Siculella, L., Sannino, A., 2017. Encapsulation of Lactobacillus kefiri in alginate microbeads using a double novel aerosol technique. Mater. Sci. Eng. C 77, 548–555.
Duhamel, R., Robert, L., Jia, H., Li, F., Lardet-Vieudrin, F., Manceau, J.-F., Bastien, F., 2006. Sensitivity of a Lamb wave sensor with 2 μm AlN membrane. Ultrasonics 44, e893–e897.
Enosawa, M., Kageyama, S., Sawai, K., Watanabe, K., Notomi, T., Onoe, S., Mori, Y., Yokomizo, Y., 2003. Use of loop-mediated isothermal amplification of the IS900 sequence for rapid detection of cultured Mycobacterium avium subsp. paratuberculosis. J. Clin. Microbiol. 41 (9), 4359–4365.
Flemming, H.-C., Wingender, J., 2010. The biofilm matrix. Nat. Rev. Microbiol. 8 (9), 623–633.
Foudeh, A.M., Daoud, J.T., Faucher, S.P., Veres, T., Tabrizian, M., 2014. Sub-femtomole detection of 16s rRNA from Legionella pneumophila using surface plasmon resonance imaging. Biosens. Bioelectron. 52, 129–135.
Foxman, B., 2010. The epidemiology of urinary tract infection. Nat. Rev. Urol. 7 (12), 653.
Fritz, J., Baller, M., Lang, H., Rothuizen, H., Vettiger, P., Meyer, E., Güntherodt, H.-J., Gerber, C., Gimzewski, J., 2000. Translating biomolecular recognition into nanomechanics. Science 288 (5464), 316–318.
Fu, Y.Q., Luo, J., Nguyen, N.-T., Walton, A., Flewitt, A.J., Zu, X.-T., Li, Y., McHale, G., Matthews, A., Iborra, E., 2017. Advances in piezoelectric thin films for acoustic biosensors, acoustofluidics and lab-on-chip applications. Prog. Mater. Sci. 89, 31–91.
Garcia, G.T., Sanchez, V.M., Marin, C.N.L., Cortez, J.I., Acevedo, C.A.R., Gonzalez, G.S. a., Ameca, J.L.H., Garcia, M.d.C.M., 2018. Wireless sensor network for monitoring physical variables applied to green technology (IoT green technology). Eur. J. Electri. Eng. Comp. Sci. 2 (2).
Grimaldi, I.A., Testa, G., Persichetti, G., Loffredo, F., Villani, F., Bernini, R., 2016. Plasma functionalization procedure for antibody immobilization for SU-8 based sensor. Biosens. Bioelectron. 86, 827–833.
Han, M., Wang, H., Yang, Y., Liang, C., Bai, W., Yan, Z., Li, H., Xue, Y., Wang, X., Akar, B., 2019. Three-dimensional piezoelectric polymer microsystems for vibrational energy harvesting, robotic interfaces and biomedical implants. Nature Electronics 2 (1), 26.
Hao, W., Liu, J., Liu, M., Liang, Y., He, S., 2016. Mass sensitivity optimization of a surface acoustic wave sensor incorporating a resonator configuration. Sensors 16 (4), 562.
He, L., Pagneux, Q., Larroulet, I., Serrano, A.Y., Pesquera, A., Zurutuza, A., Mandler, D., Boukherroub, R., Szunerits, S., 2017. Label-free femtomolar cancer biomarker detection in human serum using graphene-coated surface plasmon resonance chips. Biosens. Bioelectron. 89, 606–611.
Hobson, N., Tothill, I., Turner, A., 1996. Microbial detection. Biosens. Bioelectron. 11 (5), 455–477.
Howe, E., Harding, G., 2000. A comparison of protocols for the optimisation of detection of bacteria using a surface acoustic wave (SAW) biosensor. Biosens. Bioelectron. 15 (11–12), 641–649.
Jasson, V., Jacxsens, L., Luning, P., Rajkovic, A., Uyttendaele, M., 2010. Alternative microbial methods: an overview and selection criteria. Food microbiology 27 (6), 710–730.
Jin, H., Tao, X., Dong, S., Qin, Y., Yu, L., Luo, J., Deen, M.J., 2017. Flexible surface acoustic wave respiration sensor for monitoring obstructive sleep apnea syndrome. J. Micromech. Microeng. 27 (11), 115006.
Jin, H., Zhou, J., He, X., Wang, W., Guo, H., Dong, S., Wang, D., Xu, Y., Geng, J., Luo, J., 2013. Flexible surface acoustic wave resonators built on disposable plastic film for electronics and lab-on-a-chip applications. Sci. Rep. 3, 2140.
Kaiser, C.A., Krieger, M., Lodish, H., Berk, A., 2007. Molecular Cell Biology. WH Freeman.
Kao, K., Cheng, C., Chen, Y., Lee, Y.-H., 2003. The characteristics of surface acoustic waves on AlN/LiNbO 3 substrates. Appl. Phys. A 76 (7), 1125–1127.
Kim, J., Campbell, A.S., de Ávila, B.E.-F., Wang, J., 2019. Wearable biosensors for healthcare monitoring. Nat. Biotechnol. 1.
Kim, Y.W., Sardari, S.E., Meyer, M.T., Iliadis, A.A., Wu, H.C., Bentley, W.E., Ghodssi, R., 2012. An ALD aluminum oxide passivated Surface Acoustic Wave sensor for early biofilm detection. Sensor. Actuator. B Chem. 163 (1), 136–145.
Klein, D.C., Stroh, C.M., Jensenius, H., van Es, M., Kamruzzahan, A., Stamouli, A., Gruber, H.J., Oosterkamp, T.H., Hinterdorfer, P., 2003. Covalent immobilization of single proteins on mica for molecular recognition force microscopy. ChemPhysChem 4 (12), 1367–1371.

Konry, T., Bale, S.S., Bhushan, A., Shen, K., Seker, E., Polyak, B., Yarmush, M., 2012. Particles and microfluidics merged: perspectives of highly sensitive diagnostic detection. Microchimica Acta 176 (3–4), 251–269.
Kubitschek, H., 1990. Cell volume increase in Escherichia coli after shifts to richer media. J. Bacteriol. 172 (1), 94–101.
Lamanna, L., Rizzi, F., De Vittorio, M., Bhethanabotla, V.R., 2019a. Light Interaction with AlN-Based SAW Device Fabricated on Flexible and Silicon Substrate. 2019 IEEE SENSORS. IEEE, pp. 1–4.
Lamanna, L., Rizzi, F., Guido, F., Algieri, L., Marras, S., Mastronardi, V.M., Qualtieri, A., De Vittorio, M., 2019b. Flexible and Transparent Aluminum-Nitride-Based Surface-Acoustic-Wave Device on Polymeric Polyethylene Naphthalate. Advanced Electronic Materials, p. 1900095.
Lee, S.P., Ha, G., Wright, D.E., Ma, Y., Sen-Gupta, E., Haubrich, N.R., Branche, P.C., Li, W., Huppert, G.L., Johnson, M., 2018. Highly flexible, wearable, and disposable cardiac biosensors for remote and ambulatory monitoring. NPJ Digital Medicine 1 (1), 2.
Li, S., Wan, Y., Su, Y., Fan, C., Bhethanabotla, V.R., 2017. Gold nanoparticle-based low limit of detection Love wave biosensor for carcinoembryonic antigens. Biosens. Bioelectron. 95, 48–54.
Li, Y., Shao, M., Jiang, B., Cao, L., 2019. Surface acoustic wave pressure sensor and its matched antenna design. Measurement and Control 52 (7–8), 947–954.
Lin, C.-M., Lai, Y.-J., Hsu, J.-C., Chen, Y.-Y., Senesky, D.G., Pisano, A.P., 2011. High-Q aluminum nitride Lamb wave resonators with biconvex edges. Appl. Phys. Lett. 99 (14), 143501.
Mangayil, R., Rajala, S., Pammo, A., Sarlin, E., Luo, J., Santala, V., Karp, M., Tuukkanen, S., 2017. Engineering and characterization of bacterial nanocellulose films as low cost and flexible sensor material. ACS Appl. Mater. Interfaces 9 (22), 19048–19056.
Moll, N., Pascal, E., Dinh, D.H., Pillot, J.-P., Bennetau, B., Rebiere, D., Moynet, D., Mas, Y., Mossalayi, D., Pistré, J., 2007. A Love wave immunosensor for whole E. coli bacteria detection using an innovative two-step immobilisation approach. Biosens. Bioelectron. 22 (9–10), 2145–2150.
Niu, S., Matsuhisa, N., Beker, L., Li, J., Wang, S., Wang, J., Jiang, Y., Yan, X., Yun, Y., Burnett, W., 2019. A wireless body area sensor network based on stretchable passive tags. Nature Electronics 2 (8), 361–368.
Paton, A.W., Morona, R., Paton, J.C., 2000. A new biological agent for treatment of Shiga toxigenic Escherichia coli infections and dysentery in humans. Nat. Med. 6 (3), 265.
Pyun, J.C., Beutel, H., Meyer, J.-U., Ruf, H., 1998. Development of a biosensor for E. coli based on a flexural plate wave (FPW) transducer. Biosens. Bioelectron. 13 (7–8), 839–845.
Ranjit, N.K., Kung Jr., L., 2000. The effect of Lactobacillus buchneri, Lactobacillus plantarum, or a chemical preservative on the fermentation and aerobic stability of corn silage. J. Dairy Sci. 83 (3), 526–535.
Rao, K.S., Haumaiah, A., Sairam, P.S., 2012. Design and analysis of saw gas sensor. Eur. J. Appl. Eng. Sci. 37–42.
Rocha-Gaso, M.-I., March-Iborra, C., Montoya-Baides, Á., Arnau-Vives, A., 2009. Surface generated acoustic wave biosensors for the detection of pathogens: a review. Sensors 9 (7), 5740–5769.
Rosenberger, L.W., 2007. Modification and Characterization of Aluminum Nitride Surfaces for an Acoustic Wave Biosensor. Wayne State University.
Rusmini, F., Zhong, Z., Feijen, J., 2007. Protein immobilization strategies for protein biochips. Biomacromolecules 8 (6), 1775–1789.
Sangroniz, A., Zhu, J.-B., Tang, X., Etxeberria, A., Chen, E.Y.-X., Sardon, H., 2019. Packaging materials with desired mechanical and barrier properties and full chemical recyclability. Nat. Commun. 10 (1), 1–7.
Sanjee, S.A., Karim, M., 2016. Microbiological quality assessment of frozen fish and fish processing materials from Bangladesh. Int. J. Food Sci. 2016, 8605689, 6 pages. https://doi.org/10.1155/2016/8605689.
Shin, S.R., Zhang, Y.S., Kim, D.-J., Manbohi, A., Avci, H., Silvestri, A., Aleman, J., Hu, N., Kilic, T., Keung, W., 2016. Aptamer-based microfluidic electrochemical biosensor for monitoring cell-secreted trace cardiac biomarkers. Anal. Chem. 88 (20), 10019–10027.
Soroudi, A., Jakubowicz, I., 2013. Recycling of bioplastics, their blends and biocomposites: a review. Eur. Polym. J. 49 (10), 2839–2858.
Teonex®, Teonex® PEN film Technical Information.
Venkatachalam, S., Nayak, S.G., Labde, J.V., Gharal, P.R., Rao, K., Kelkar, A.K., 2012. Degradation and Recyclability of Poly (Ethylene Terephthalate). InTech India, Polyester, pp. 75–98.
Wang, T., Green, R., Nair, R.R., Howell, M., Mohapatra, S., Guldiken, R., Mohapatra, S.S., 2015. Surface acoustic waves (SAW)-based biosensing for quantification of cell growth in 2D and 3D cultures. Sensors 15 (12), 32045–32055.
Watnick, P., Kolter, R., 2000. Biofilm, city of microbes. J. Bacteriol. 182 (10), 2675–2679.
Xiao, Y., Isaacs, S.N., 2012. Enzyme-linked immunosorbent assay (ELISA) and blocking with bovine serum albumin (BSA)—not all BSAs are alike. J. Immunol. Methods 384 (1–2), 148–151.
Xu, S., 2012. Electromechanical biosensors for pathogen detection. Microchimica Acta 178 (3–4), 245–260.
Zardetto, V., Brown, T.M., Reale, A., Di Carlo, A., 2011. Substrates for flexible electronics: a practical investigation on the electrical, film flexibility, optical, temperature, and solvent resistance properties. J. Polym. Sci. B Polym. Phys. 49 (9), 638–648.
Zhou, J., Pang, H.-F., Garcia-Gancedo, L., Iborra, E., Clement, M., De Miguel-Ramos, M., Jin, H., Luo, J., Smith, S., Dong, S., 2015. Discrete microfluidics based on aluminum nitride surface acoustic wave devices. Microfluid. Nanofluidics 18 (4), 537–548.